Haddad, H.; Jodeau, M.; Claude, N.; Antoine, G.; Legout, C.

Fine sediment deposits in gravel bed rivers: sensitivity analysis to particle properties using a 2D hydrodynamic and sediment model

Fine sediment deposits in gravel bed rivers: sensitivity analysis to particle properties using a 2D hydrodynamic and sediment model

H. Haddad, M. Jodeau, N. Claude & G. Antoine
National Hydraulics and Environment Laboratory (LNHE)
EDF R&D
Chatou, France
hanna.haddad@edf.fr

C. Legout
Université Grenoble Alpes, CNRS, IRD, Grenoble INP,
IGE, Grenoble, France

***Abstract*— Fine sediment dynamics in mountainous rivers are poorly understood. However, high suspended sediment concentrations during natural events or reservoir flushing are known to be an issue further downstream. Numerical models are frequently used to predict sediment behavior, but measurements of cohesive sediment properties are rarely available. This study investigates the sensitivity of a numerical model to parameters describing cohesive sediment behavior. The study case is a 3-km reach of the Isère River in the Alps with alternate gravel bars. The simulated outputs are the surfaces and volumes of fine sediment deposits over control areas. These outputs are analyzed to assess the sensitivity to the parameters describing erosion and sedimentation in order to identify on which measurements and in which areas measurements efforts should be focused. For two simulated flushing events, disparities between various deposition areas are observed, depending on their locations on the gravel bar and the local hydraulic conditions.**

I. INTRODUCTION

Fine sediments exhibit various stages of deposition and erosion during their transport from hillslopes to the ocean [1]. In alpine gravel bed rivers, massive deposits can occur, leading to bar elevation, riparian vegetation growth and consequently to bar stabilization, which in turn increases flooding risks and alters the river ecological quality [2]. Hydropower dams modify fine sediment fluxes in downstream rivers. While the presence of cohesive sediment deposits is highly visible in such environments, the processes leading to their deposition and potential resuspension is poorly understood. This is particularly due to the high spatial and temporal variability of fine sediment deposits characteristics [3] in preferential deposition areas [4].

Distributed numerical models are interesting tools to better understand cohesive sediment dynamics and to predict sediment propagation, transport and deposition during a period of interest. Multiple studies investigated the efficiency of various operations on the river, including flushing flows [5], [6] and dredging operations [7]. A few of them focused on spatial and temporal variations of fine sediment properties [8], [9]. However, in many numerical studies, measurements of cohesive sediment properties are not available [10]. Thus, one has to use values from the literature often obtained for different conditions or to perform calibrations. The aim of this study is to assess i) the capability of a 2D numerical model to reproduce fine sediment deposits on gravel bars, ii) which parameters describing erosion and sedimentation of cohesive particles are the most sensitive and iii) to which extent the results of sensitivity analysis are controlled by global boundary and local hydrodynamic conditions.

II. MATERIAL AND METHODS

A. Study site

1) Fréterive reach on the Isère river

The Isère River is a gravel bed river located in the southern French Alps. The modeled area is a 3 km reach located 38 km downstream the Aigueblanche dam and 200 m upstream of the Isère-Arc confluence. It is embanked, rectilinear and about 100 m wide, with a bed slope of 0.0016 m/m. Bed material is composed of coarse sediment (d_{50} =24 mm), non-cohesive fine sediment (d_{50} =180 µm) and cohesive sediment (d_{50} =40 µm). The average suspended sediment concentration (SSC) is less than 1 g/l most of the time but can reach more than 10 g/l during runoff or flushing events of the Aigueblanche dam.

During the 2017 winter, the area was subject to restoration works that consisted of mechanically removing vegetation and fine sediments from gravel bars as well as remodeling the gravel bars. These operations were performed to reduce the flooding risk and restore the bar mobility.

2) The 2017 and 2018 flushing events of the Aigueblanche dam

The Aigueblanche dam is flushed once a year if the spring discharges are high enough. This operation allows to remove fine sediment in the reservoir to limit the transfer of sand to the turbine and the elevation of the bed river upstream of the reservoir. The 2017 and 2018 flushing events were characterized by distinct maximal liquid discharge and sediment concentration. Thus, these two events were selected to investigate differences in terms of deposition and erosion.

The 2017 flushing event (fig 1.a) lasted 3 days (28/05 to 31/05), with a liquid discharge peak of 200 m^3/s and a SSC peak of 12 g/l with a 1-day delay compared to the peak discharge.

The 2018 flushing event starting from 06/05/2018 (fig 1.b) lasted 3 days and reached higher discharges (peak discharge around 300 m^3/s) with smaller SSC. The modelled event includes the flushing and can be decomposed in three parts. The main SSC peak, around 2.5 g/l was reached 8 hours after the peak discharge. In a second part, a flood event (starting from 09/05/2018) corresponds to a rinsing test that was performed to try to limit the fine sediment deposits after the flushing event. The goal of these high discharges was to re-suspend eventual deposits on downstream gravel bars. These events were followed by a natural runoff event with high discharges.

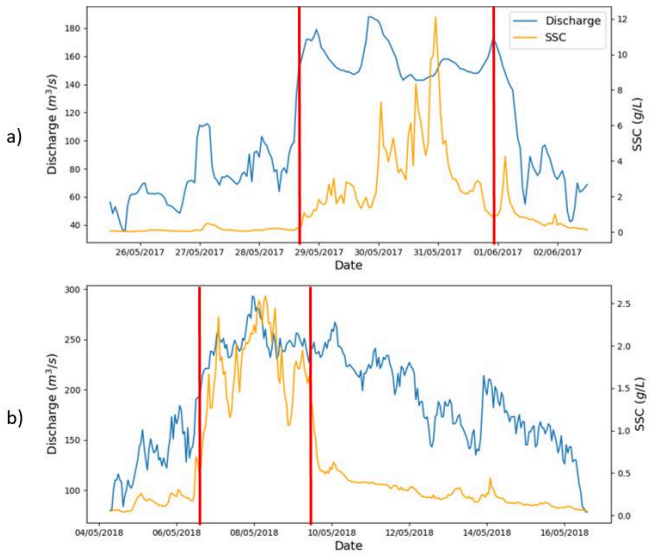

Figure 1. Discharge and suspended sediment concentrations (SSC) for two flushing events in (a) 2017 and (b) 2018. Vertical red lines correspond to the flushing period for each modelled event.

3) Bed elevation data and aerial pictures

Topography and bathymetry surveys were performed between January and April 2017 as well as a LIDAR (Light Detection and Ranging) measurements in 2014. They were used to create the digital elevation model (DEM) of the Fréterive reach. Four aerial photos, two in April and May before the 2017 flushing event and two in June and July after the 2017 flushing, are available. The comparison of manually digitized contours of fine deposit patches on the photos allows to obtain the surfaces of fine sediment deposits before and after the flushing event on the gravel bars for a given discharge.

While the modeled reach is 3km long, the sensitivity analysis focuses only on 2 bars (fig 2) representative of the whole reach. In this zone, multiple areas of deposits are identified from aerial photography: a secondary channel (named SC), 5 marginal deposits on the right bank of the central bar (RBMDi with i from 1 to 5), 3 on the left bank (LBMDi with I from 1 to 3) and 2 bar tail deposits, BTI4 and BTU4. Control areas were chosen for each of these areas.

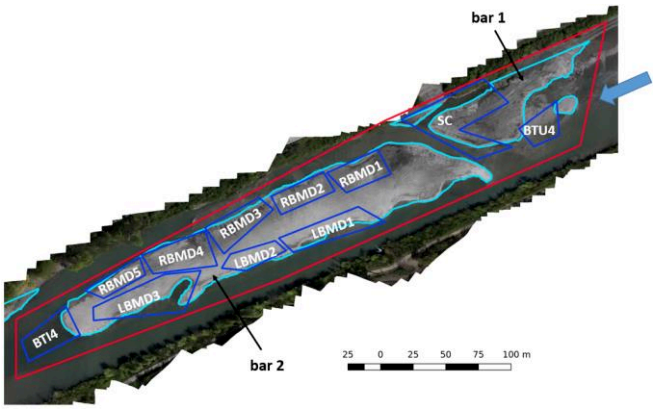

Figure 2. Area of interest illustrated by a photography taken in April 2017 ($Q=35\ m^3/s$) after the restoration works and before the flushing event of 2017. Bars are digitized in light blue. The blue arrow indicates the water direction from right to left. The contour in red covers the whole area and the blue ones are the areas of various patches: right bank marginal deposit (RBMD), left bank marginal deposit (LBMD), bar tails (BTI4 and BTU4) and secondary channel (SC).

B. Modeling of the Fréterive site

The numerical simulations were run using the release 8.0 of TELEMAC-2D and SISYPHE from the open source TELEMAC-MASCARET hydro-informatics system coupled with SISYPHE [11]–[13]. The model includes 526,653 nodes and 1,042,620 triangular mesh elements. The mean node distance is about 1.6m. The model simulation time step has been set to 1 s in order to respect the Courant-Friedrichs-Lewy (CFL) condition.

For all the calculations, the initial bed elevation corresponds to the configuration before the 2017 flushing event (remodeled bars without fine sediment deposits).

1) Hydraulics and calibration of the Strickler coefficient

The boundary conditions for the hydraulics are the following: for a prescribed liquid discharge at the inlet of the domain, a Manning-Strickler law is used to compute the water level at the outlet of the modeled area, with the approximation of a wide rectangular canal. The mean slope is obtained from the measured bathymetry. The Strickler coefficient was calibrated to 40 $m^{1/3}/s$ allowing to reproduce at best the modeled surfaces of non-immersed gravel bars obtained with aerial photography observations for two steady states ($Q=35\ m^3/s$ in April and $Q=53\ m^3/s$ in May).

2) Sediment transport

In this study case, two main hypothesis were taken, given the configuration of the study site: (1) bed load is not taken into account, for the 2017 flushing event, data show that the bed evolution due to bed load is negligible. (2) It should be stressed that the input SSC shown in figure 1 is a mixture of all sediments. Since no data on the suspended sediment classes is available, the sedigraph is modeled considering a unique class of cohesive sediment with given properties (settling velocity, critical erosion and deposition shear stresses and erosion rate). The Partheniades and Krone formulae are used to compute the erosion and deposition flux:

$$E = \begin{cases} M\left[\left(\frac{\tau_b}{\tau_{ce}}\right) - 1\right] & if\ \tau_b > \tau_{ce} \\ 0 & otherwise \end{cases} \quad (1)$$

$$D = \begin{cases} w_s C\left[1 - \frac{\tau_b}{\tau_{cd}}\right] & if\ \tau_b < \tau_{cd} \\ 0 & otherwise \end{cases} \quad (2)$$

where E is the erosion flux [kg/m^2/s], M the Partheniades constant [kg/m^2/s], τ_b the bottom shear stress [Pa], τ_{ce} the critical erosion shear stress [Pa]. D is the deposition rate [kg/m^2/s], w_s the settling velocity [m/s], C the depth-averaged concentration [kg/m3] and τ_{cd} the critical shear stress for deposition [Pa].

3) Sensitivity study methodology

Multiple field and laboratory measurements were conducted previously on the Isère River and other similar gravel bed rivers in the Alps. They were used to define the range of values for each parameter describing the sediment properties. Table 1 shows the chosen values for the reference simulation. The settling velocity and the critical erosion shear stress were derived from mean values extracted from the measurements [3]. The values of the critical deposition shear stress and the erosion rate M were chosen as an approximation since no measurement is available.

First of all the aerial photos after the 2017 flushing event are used to check if the model correctly reproduced the locations and surfaces of deposits for the reference simulation. Then, one parameter at a time is modified and values are tested for multiple orders of magnitude in order to test the sensitivity of the modeled outputs. The 2017 and 2018 flushing events are simulated in order to assess the effect of different upstream boundary conditions.

TABLE 1. LIST OF SIMULATIONS FOR THE COHESIVE SENSITIVITY STUDY. EACH PARAMETER WAS VARIED FOR A WIDE RANGE OF VALUES (COLUMNS 3) TO TEST ITS INFLUENCE OVER MULTIPLE ORDERS OF MAGNITUDE.

Parameter	Reference simulation	Min and Max values for the sensitivity analysis
w_s[m/s]	$0.17.10^{-3}$	[10^{-5} → 10^{-2}]
τ_{cd} [Pa]	0.4	[10^{-3} → 40]
τ_{ce} [Pa]	1	[0.1 → 6]
M [kg/m^2/s]	10^{-3}	[10^{-4} → 1]

To evaluate the model sensitivity for given boundary conditions, the volume of deposit is calculated for each control area (fig 2) or for the whole area. Plotting the dimensionless volume Y against the dimensionless parameter X shows the sensitivity. A higher gradient indicates a more sensitive parameter.

$$X = \frac{parameter\ value}{reference\ value\ of\ the\ parameter} \quad (3)$$

$$Y = \frac{deposit\ volume}{reference\ deposit\ volume} \quad (4)$$

III. RESULTS AND DISCUSSION

A. Evaluation of the sediment model

The first step was to evaluate the model's capability to reproduce fine sediment deposits. Thus, the model was tested for the 2017 flushing event for cohesive sediments using the reference simulation configuration. The observed surfaces of deposits are derived from the aerial photography taken in July 2017 at low discharge after the flushing event. Figure 3 represents the observed and simulated deposits over the two gravel bars.

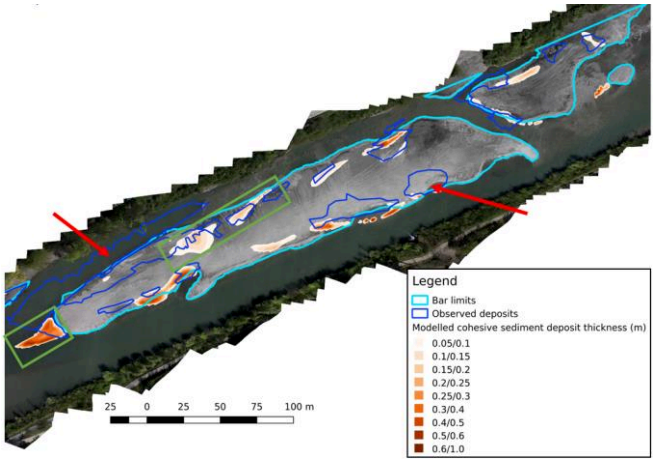

Figure 3. Map of observed and modeled deposits in the area with the reference configuration for cohesive sediment. For the modeled outputs, the legend starts for a deposit value of 0.05m: a deposit is only considered if it is higher than 0.05 m. Red arrows indicate numerical errors in locations related to interpolation and lack of topography measurements. Green rectangles show bar tail deposits thicker than superficial deposits.

The total surface of the observed deposits in the area is 5400 m^2 and the numerical model reproduces 2550 m^2. About half of the observed deposits are not reproduced by the model. However, aerial photography observations include sandy areas as well as cohesive deposits and cannot be distinguished. The model focuses only on cohesive sediment and it is therefore normal to reproduce less deposits than the observed ones. Furthermore, some numerical errors are related to interpolation of topography on the central bar as well as a lack of measurements in the channel on the right of the central bar (red arrows on figure 3).

Nevertheless, marginal deposits, bar tail deposits, secondary channel deposits as well as superficial deposits, can be identified. This is coherent with the description of deposits given by Wood and Armitage [14] and observed by Gregory et al. [4].

The thickness of different deposits is not available. However, the numerical model is in agreement with field observations that show that bar tail deposits are thicker than marginal and superficial ones. The reference simulation leads to a maximum of more than 40 cm of deposits on the bar tail and less than 10 cm in some superficial areas (green rectangles on figure 3).

It is thus fair to say that the model reproduces quite well cohesive sediment deposits in the zone.

B. *Global sensitivity analysis*

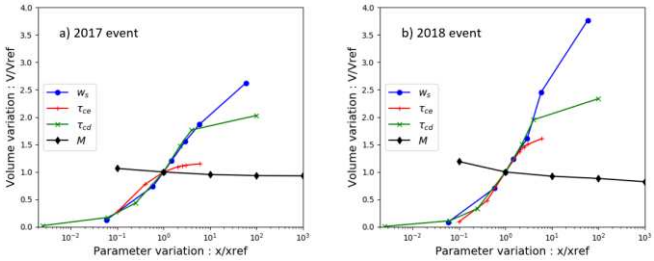

Figure 4. Sensitivity to cohesive sediment parameters in the whole area for the (a) 2017 flushing event and (b) 2018 flushing event.

For the global sensitivity analysis, the dimensionless volumes are plotted according to the four dimensionless parameters (fig 4).

For the 2017 flushing event, the reference deposit volume in the zone is 423.04 m^3 (table 2). This volume is multiplied by 2.6 when the settling velocity is 2 orders of magnitude higher and divided by 8 when the settling velocity is one order of magnitude lower (fig 4.a, blue line, and table 2). The plot for the critical shear stress for deposition (fig 4.a, green line) follows the same slope except for the last point. For this event, these parameters are the most sensitive ones. The critical erosion shear stress is less sensitive than w_s and τ_{cd} but plays a non-negligible role: the minimum volume obtained is 115 m^3 and the maximum 486 m^3. This suggests that the higher the value of τ_{ce} is, the more fine sediments are re-suspended. A threshold is reached for the high values of τ_{ce}, which suggests that the highest values for bed shear stress obtained for these boundary conditions are lower than the threshold.

For the 2018 flushing event, the reference simulation leads to a total volume of deposit of 401.5 m^3 which is 5% lower than the volume simulated with the 2017 event (table 2). The 2018 flushing event exhibits higher discharges and thus globally higher shear stresses. This leads to less deposits. The settling velocity and critical shear stress for deposition are also very sensitive for the 2018 event. But also, for the 2018 boundary conditions, the outputs are more sensitive to the critical erosion shear stress than for the other event (fig 4.b, red line): the maximum and minimum volumes are respectively 644 m^3 and 37 m^3, values which are more spread out than for the 2017 event and the slope of the line is higher. τ_{ce} is a very sensitive parameter for higher discharges and is as sensitive as w_s and τ_{cd} for the second scenario tested.

TABLE 2. DEPOSITED REFERENCE VOLUME FOR EACH EVENT AND MIN AND MAX DEPOSITED VOLUME FOR EACH PARAMETERS

Deposited volume (m^3)	2017		2018	
	min	max	min	max
Reference	423.04		401.5	
w_s	54	1110	35	1512
τ_{cd}	10	859	4	938
τ_{ce}	115	486	37	644
M	393	451	330	478

C. *Effect of local hydraulic conditions*

These conclusions derived at the bar scale might exhibit spatial variations depending on the location in the bar. Thus, the sensitivity was investigated at smaller scales corresponding to various facies of deposition areas, i.e. RBMD1, BTI and SC.

For the 2017 flushing event, in RBMD1 (fig 5.a) and SC (fig 5.c) the reference volumes are respectively 28 m^3 and 36 m^3. In RBMD1 τ_{cd} is the most sensitive parameter (volume multiplied by 3 when τ_{cd} is multiplied by 4) followed by w_s (volume multiplied by 3 when w_s is multiplied by 100). In the SC area (fig 5.c), the settling velocity is the most sensitive parameter (volume multiplied by 5 for maximum value, outside graph) while τ_{ce} and τ_{cd} are equally sensitive.

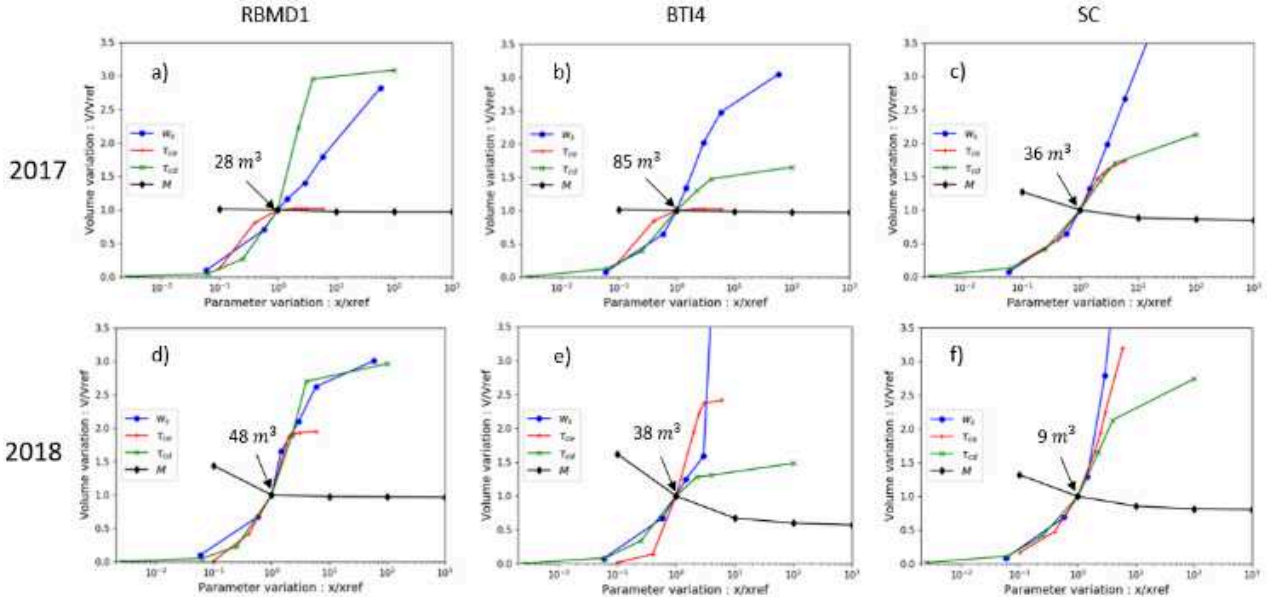

Figure 5. Sensitivity on different control volumes for the (a,b and c) 2017 and (d,e and f) 2018 events.
The y axis is limited between 0 and 3.5 in order to compare the different figures, maximum values don't appear on the plots (e) and (f).

The results can be compared to two studies. Hostache et al. [9] looks at general sensitive parameters on a large floodplain scale and evidence the fact that the most sensitive parameter is the settling velocity which is coherent with figure 4. Our study's objectives are however closer to the ones aimed by Milan et al. [15] where they look at spatial patterns in sediment deposit related to hydraulic conditions and velocities. Indeed, the spatial differences observed in figure 5 can be explained by local hydraulic conditions related to gravel bed topography. For the same global boundary conditions, local velocities are controlled by topography and can favor one parameter of the sediment over another. The results suggest that on high altitudes (superficial part of gravel bars), shear stresses are low and therefore τ_{cd} is a very sensitive parameter. On low altitudes w_s and τ_{ce} gain more importance.

By comparing the 2017 and 2018 flushing events, we can notice that the global boundary condition can sharpen the difference in sensitivity in different areas. For the 3 control volumes in figure 5, the critical erosion shear stress is much more sensitive for the 2018 boundary conditions than for the 2017 ones. In the bar tail area for example, τ_{ce} is the most sensitive parameter for the 2018 event (volume multiplied by 2.5 and divided by 9 when the parameter is respectively multiplied by 3 and divided by 2), at least before the threshold is reached.

Figures 4 and 5 show that the critical shear stress for deposition is a very sensitive coefficient. This can be a source of uncertainty in modeling studies since direct measurement of this quantity is not possible in situ. However, in the community, the existence of this variable is debated [16]. Indeed, some authors argue that deposition and erosion occur at the same time [17]. In fact, on the plots in figures 4 and 5, a "break" in the slope of the green line is clearly visible when τ_{cd} becomes larger than τ_{ce}, which corresponds to a change of paradigm and deposition and erosion are allowed at the same time.

IV. Conclusions

The aim of this study was to better understand the behavior of fine sediment deposits in a 2D morphodynamic numerical model for two different flushing events in a gravel bed river.

The main results are: (1) the simulated deposition map exhibits good agreement with observed fine sediment deposits with parameters estimated from previous in situ measurements. (2) An event with higher discharges intensifies the sensitivity to the critical erosion shear stress. (3) Local topography and hydraulic conditions are important factors to the sensitivity of the modeled deposits to cohesive sediment parameters.

These results highlight the importance of knowing sediment origins and their properties and will be considered during future field monitoring seeking to supply the numerical model.

Acknowledgements

The authors would like to thank the French National Reasearch Agency (ANR) under the grant ANR-18-CE01-0020 (DEAR project) and EDF CIH for their support.

References

[1] K. Fryirs, "(Dis)Connectivity in catchment sediment cascades: a fresh look at the sediment delivery problem" Earth Surface Processes and Landforms, vol. 38, no. 1, pp. 30–46, Jan. 2013, doi: 10.1002/esp.3242.

[2] C. Jourdain, N. Claude, P. Tassi, F. Cordier, and G. Antoine, "Morphodynamics of alternate bars in the presence of riparian vegetation," Earth Surface Processes and Landforms, Dec. 2019, doi: doi: 10.1002/esp.4776.

[3] C. Legout, I. G. Droppo, J. Coutaz, C. Bel, and M. Jodeau, "Assessment of erosion and settling properties of fine sediments stored in cobble bed rivers: the Arc and Isère alpine rivers before and after reservoir flushing: Erosion and settling dynamics of fine sediments in cobble bed rivers," Earth Surf. Process. Landforms, vol. 43, no. 6, pp. 1295–1309, May 2018, doi: 10.1002/esp.4314.

[4] B. Camenen, M. Jodeau, and M. Jaballah, "Estimate of fine sediment deposit dynamics over a gravel bar using photography analysis," International Journal of Sediment Research, vol. 28, no. 2, pp. 220–233, Jun. 2013, doi: 10.1016/S1001-6279(13)60033-5.

[5] A. Gregory, R. R. Morrison, and M. Stone, "Assessing the Hydrogeomorphic Effects of Environmental Flows using Hydrodynamic Modeling," Environmental Management, vol. 62, no. 2, pp. 352–364, Aug. 2018, doi: 10.1007/s00267-018-1041-6.

[6] T. Esmaeili, T. Sumi, S. Kantoush, Y. Kubota, S. Haun, and N. Rüther, "Three-Dimensional Numerical Study of Free-Flow Sediment Flushing to Increase the Flushing Efficiency: A Case-Study Reservoir in Japan," Water, vol. 9, no. 11, p. 900, Nov. 2017, doi: 10.3390/w9110900.

[7] M. Haimann et al., "Monitoring and modelling concept for ecological optimized harbour dredging and fine sediment disposal in large rivers," Hydrobiologia, vol. 814, no. 1, pp. 89–107, Jun. 2018, doi: 10.1007/s10750-016-2935-z.

[8] M. Tritthart, M. Haimann, H. Habersack, and C. Hauer, "Spatio-temporal variability of suspended sediments in rivers and ecological implications of reservoir flushing operations," River Res Applic, vol. 35, no. 7, pp. 918–931, Sep. 2019, doi: 10.1002/rra.3492.

[9] R. Hostache, C. Hissler, P. Matgen, C. Guignard, and P. Bates, "Modelling suspended-sediment propagation and related heavy metal contamination in floodplains: a parameter sensitivity analysis," Hydrol. Earth Syst. Sci., vol. 18, no. 9, pp. 3539–3551, Sep. 2014, doi: 10.5194/hess-18-3539-2014.

[10] R. C. Grabowski, I. G. Droppo, and G. Wharton, "Erodibility of cohesive sediment: The importance of sediment properties," Earth-Science Reviews, vol. 105, no. 3–4, pp. 101–120, Apr. 2011, doi: 10.1016/j.earscirev.2011.01.008.

[11] R. Ata, "Telemac user manual." Dec. 2018.

[12] P. Tassi, "Sisyphe user manual." Dec. 2018.

[13] C. Villaret, J.-M. Hervouet, R. Kopmann, U. Merkel, and A. G. Davies, "Morphodynamic modeling using the Telemac finite-element system," Computers & Geosciences, vol. 53, pp. 105–113, Apr. 2013, doi: 10.1016/j.cageo.2011.10.004.

[14] P. J. Wood and P. D. Armitage, "Sediment deposition in a small lowland stream-management implications," p. 12, 1999.

[15] D. Milan, G. Heritage, N. Entwistle, and S. Tooth, "Morphodynamic simulation of sediment deposition patterns on a recently stripped bedrock anastomosed channel," Proc. IAHS, vol. 377, pp. 51–56, Apr. 2018, doi: 10.5194/piahs-377-51-2018.

[16] J. P.-Y. Maa, J.-I. Kwon, K.-N. Hwang, and H.-K. Ha, "Critical Bed-Shear Stress for Cohesive Sediment Deposition under Steady Flows," J. Hydraul. Eng., vol. 134, no. 12, pp. 1767–1771, Dec. 2008, doi: 10.1061/(ASCE)0733-9429(2008)134:12(1767).

[17] J. C. Winterwerp, W. G. M. van Kesteren, B. van Prooijen, and W. Jacobs, "A conceptual framework for shear flow-induced erosion of soft cohesive sediment beds" J. Geophys. Res., vol. 117, no. C10, p. n/a-n/a, Oct. 2012, doi: 10.1029/2012JC008072.